Sevoflurane-Induced miR-211-5p Promotes Neuronal Apoptosis by Inhibiting Efemp2

Yousu Shen[1,*], Tao Zhou[1,*], Xiaobing Liu[1], Yanlong Liu[1], Yaqi Li[1], Dewu Zeng[1], Wensheng Zhong[1] and Mingsheng Zhang[1]

Abstract

Sevoflurane exposure can result in serious neurological side effects including neuronal apoptosis and cognitive impairment. Although the microRNA miR-211-5p is profoundly upregulated following sevoflurane exposure in neonatal rodent models, the impact of miR-211-5p on neuronal apoptosis and cognitive impairment postsevoflurane exposure has not yet been elucidated. Here, we found that sevoflurane upregulated miR-211-5p and downregulated EGF-Containing Fibulin Extracellular Matrix Protein 2 (Efemp2, Fibulin-4) levels in vitro and in vivo. Sevoflurane's effect on miR-211-5p expression was based on enhancing primary miR-211 transcription. miR-211-5p targets Efemp2's mRNA 3′-untranslated region, reducing Efemp2 expression. RNA immunoprecipitation revealed significant enrichment of the miR-211-5p:Efemp2 mRNA dyad in the RNA-induced silencing complex. miR-211-5p mimics downregulated Efemp2, leading to phosphorylation of Smad2 and Smad3, upregulation of pro-apoptotic Bim, and mitochondrial release of allograft inflammatory factor 1 and cytochrome C. In contrast, miR-211-5p hairpin inhibitor (AntimiR-211-5p) negatively regulated this apoptotic pathway and reduced neuronal apoptosis in an Efemp2-dependent manner. Sevoflurane-exposed mice administered AntimiR-211-5p displayed reduced cortical apoptosis levels and near-term cognitive impairment. In conclusion, sevoflurane-induced miR-211-5p promotes neuronal apoptosis via Efemp2 inhibition. Summary statement: This study revealed the significance of sevoflurane-induced increases in miR-211-5p on the promotion of neuronal apoptosis via inhibition of Efemp2 and its downstream targets.

Introduction

Sevoflurane is regularly employed as an inhaled pediatric and adult anesthetic in the clinic due to its quick induction and recovery time and low blood/gas partition coefficient (Brioni et al., 2017). However, two prospective randomized parallel-group clinical trials have shown that sevoflurane exposure can advance postoperative cognitive dysfunction in adults (Liu et al., 2013a; Qiao et al., 2015). In pediatric patients, brain structure and neurocognitive development have been shown to be directly altered by sevoflurane, resulting in an elevated possibility of cognitive dysfunction (Backeljauw et al., 2015; Sun 2010; Vutskits & Xie, 2016). Moreover, previous studies in neonatal and adult animal models have linked sevoflurane inhalation to enhanced neuronal apoptosis (Chen et al., 2013; Liu et al., 2013b; Qiu et al., 2015; Zheng et al., 2013) and cognitive deficits (Jiang et al., 2017; Liu et al., 2013a; Satomoto et al., 2009; Takaenoki et al., 2014; Tao et al., 2014; Yu et al., 2016). Unfortunately, the mechanisms underlying sevoflurane-induced neurotoxicity and cognitive dysfunction have not been fully investigated.

MicroRNAs (miRNAs) are a class of small (20–23 nucleotides) noncoding RNAs which promote posttranslation suppression of gene expression. miRNAs attach to the 3′-untranslated region (UTR) of mRNAs resulting in inhibition of their translation and/or their degradation. miRNAs have been linked to the regulation of apoptotic pathways in neuronal cells (Jimenez-Mateos & Henshall, 2013) and the

[1]Department of Anaesthesiology, Jiangxi Provincial People's Hospital Affiliated to Nanchang University, Jiangxi, China

*Yousu Shen and Tao Zhou contributed equally to this work.

Corresponding Author:
Mingsheng Zhang, Department of Anaesthesiology, Jiangxi Provincial People's Hospital Affiliated to Nanchang University, No. 92 Aiguozhe Street, Nanchang City, Jiangxi 330006, China.
Email: zms9201@126.com

development of central nervous system disorders (Liu et al., 2010; Redell et al., 2009; Ziu et al., 2011). Although several miRNAs are profoundly upregulated following sevoflurane exposure in neonatal rodent models (e.g., miR-211, miR-632, miR-466b-1-3p, miR-196c-3p) (Fujimoto et al., 2015; Ye et al., 2016), the association between these key candidate miRNAs and the mechanisms behind sevoflurane-induced neurotoxicity and cognitive dysfunction have not been thoroughly investigated.

This study investigated whether apoptosis-related cell loss and cognitive deficits can be linked to sevoflurane-induced upregulation of the key candidate miRNA miR-211-5p. An increase in miR-211-5p expression was revealed in the brain during the 72-h period postsevoflurane exposure. In vivo and in vitro models were employed to show that miR-211-5p affects neuronal apoptosis postsevoflurane exposure via inhibition of EGF-Containing Fibulin Extracellular Matrix Protein 2 (Efemp2, Fibulin-4). Treatment with a miR-211-5p hairpin inhibitor (AntimiR-211-5p) reversed these negative effects.

Materials and Methods

Animals

This study was approved by the Ethics Committee of [hospital name] ([city name], [country]). The guidelines detailed in the Guide for the Care and Use of Laboratory Animals (NIH 85-23-2985) were adhered to during all animal procedures. The experimental procedures are fully detailed in the Supplementary Methods. PRISM version 6 was used to perform all statistical analyses (GraphPad Software, La Jolla, CA, USA). If the data was shown to have a normal distribution, either unpaired Student's *t*-testing, one-way analysis of variance (ANOVA) with Tukey post-hoc testing, or two-way ANOVA (condition [room air, sevoflurane, etc.] × treatment [AntimiR-Ctrl, AntimiR-211-5p, etc.]) with Tukey post-hoc testing were applied as indicated. The *y*-axis labels indicate the control groups used for each comparison.

Results

Rapid Upregulation of Pro-Apoptotic miR-211-5p at the Transcriptional Level by Sevoflurane

To assess the effects of sevoflurane on miR-211-5p expression in vivo, we exposed mice to 5% sevoflurane or sham conditions (room air) mice for 4 h. As previously shown in neonatal rat brains (Fujimoto et al., 2015), miR-211-5p expression was significantly upregulated in the murine brain following sevoflurane exposure (Figure 1a). A rapid increase in miR-211-5p was observed as early as 1 h postsevoflurane exposure; this increase peaked at 6 h and was maintained at 72 h postsevoflurane exposure (Figure 1a). To assess the effects of sevoflurane on miR-211-5p expression in cortical neurons in vitro, we exposed primary rat cortical neurons

(RCNs) to 3.4% sevoflurane or room air for three hours. Two in vitro models of cortical neuronal apoptosis, staurosporine and etoposide (Sabirzhanov et al., 2012), were employed as positive controls for apoptosis. RCNs were selected over murine cortical neurons due to their superior robustness under excitotoxic stress in vitro (Cunha-Oliveira et al., 2006; Nassogne et al., 1998; Yang et al., 2010; Yu et al., 1999). miR-211-5p levels were significantly increased at 3 h following sevoflurane exposure (Figure 1b). miR-211-5p levels were also significantly increased by 3 h after induction of apoptosis in both the etoposide and staurosporine models (Figure 1b).

The transcriptional inhibitor α-amanitin (α-Am) was used to investigate the rapid increase in miR-211-5p levels in response to sevoflurane exposure. Quantitative polymerase chain reaction (qPCR) was used to assess expression of primary miRNA-211 (pri-miR-211) and mature miR-211-5p in RCNs treated with room air or sevoflurane at 1, 3, and 6 h post-α-Am treatment (10 μg/mL). Inhibition of miR-211-5p transcription by α-Am under room air conditions caused rapid reductions in pri-miR-211 and mature miR-211-5p levels (Figure 1c). pri-miR-211 and mature miR-211-5p levels rapidly increased following sevoflurane exposure (Figure 1d). The addition of α-Am caused rapid reductions in pri-miR-211 and mature miR-211-5p levels, implying the role of enhanced transcription in sevoflurane's induction of miR-211-5p (Figure 1e). A similar pattern of findings were found in the positive control etoposide model (Figure 1c to e). These results reveal that sevoflurane's effect on miR-211-5p expression is based on enhancing pri-miR-211 transcription.

The regulation of RCN apoptosis by miR-211-5p was assessed with miR-211-5p mimics. Apoptosis, as measured by lactate dehydrogenase (LDH) release and cleaved caspase-3 (CC-3) activity, was increased by miR-211-5p mimics in a dosage-dependent manner (Figure 1f and g). In order to assess whether miR-211-5p inhibition would impact sevoflurane-induced apoptosis, RCNs were transfected with a miR-211-5p hairpin inhibitor or control hairpin inhibitor (AntimiR-211-5p or AntimiR-Ctrl, respectively) and exposed to sevoflurane. AntimiR-211-5p significantly decreased sevoflurane-induced LDH release and CC-3 activity in a dosage-dependent manner (Figure 1h and i). A similar pattern of findings were found in the positive control etoposide and staurosporine models (Figure 1f to i).

Sevoflurane-Induced Neuronal Apoptosis Rescued by AntimiR-211-5p In Vitro

The effect of miR-211-5p inhibition on neuronal apoptosis was further assessed via transfection of RCNs with AntimiR-211-5p or AntimiR-Ctrl prior to room air or sevoflurane exposure and subsequent Western blot analysis of apoptosis markers (Figure 2a). Sevoflurane exposure
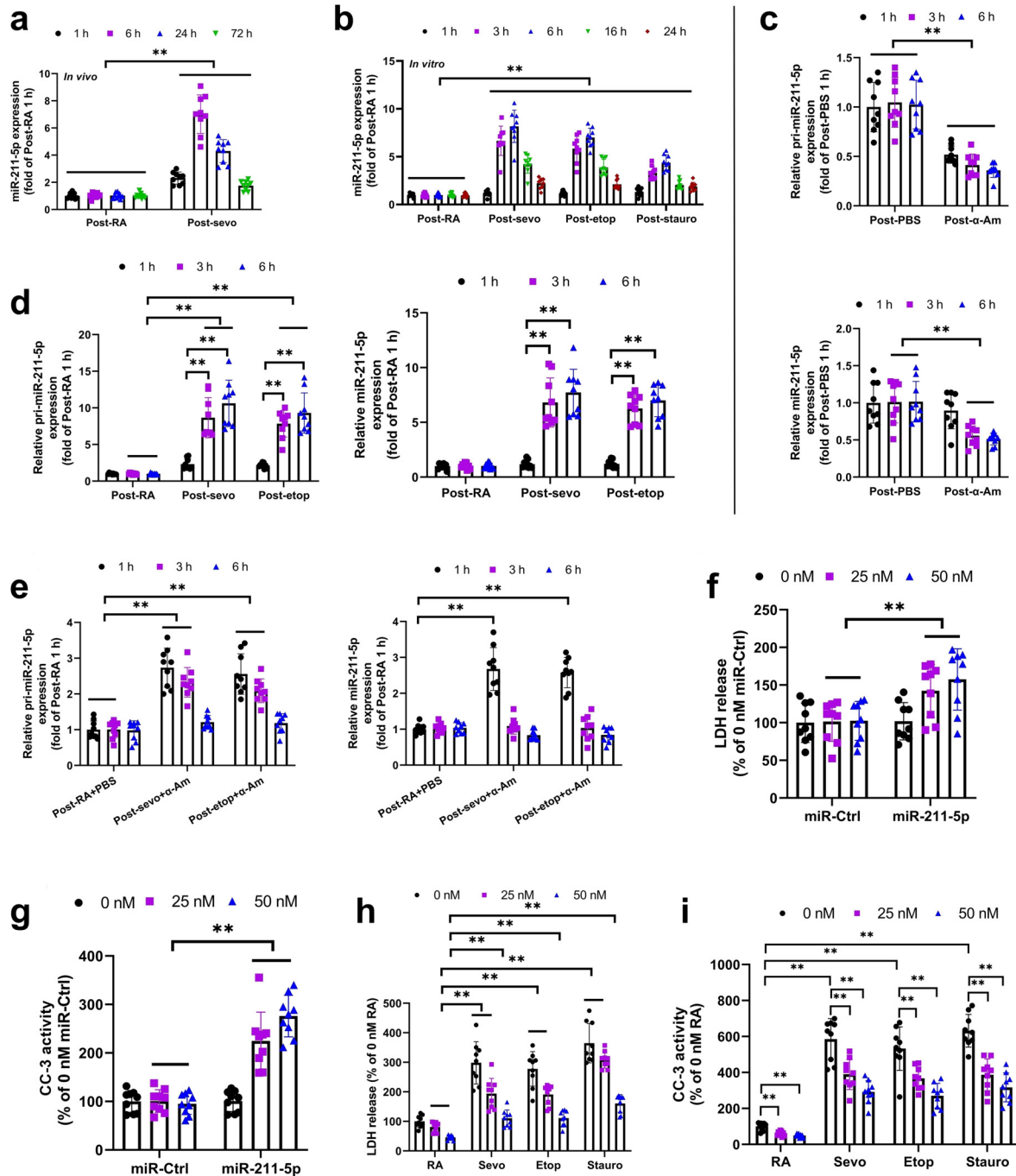
Figure 1. Rapid upregulation of miR-211-5p at the transcriptional level by sevoflurane. (a) qPCR quantification of in vivo cortical miR-211-5p levels 72 h following RA or sevoflurane exposure ($n = 9$ mice per cohort). (b) qPCR quantification of in vitro miR-211-5p levels in primary RCNs after treatment with RA, sevoflurane, etoposide, or staurosporine. (c) RCNs were cultured with 10 μg/mL α-Am; qPCR was then used to analyze levels of pri-miR-211-5p (top) and miR-211-5p (bottom) at 1, 3, and 6 h after α-Am treatment. (d) RCNs were cultured with RA, sevoflurane, etoposide, or staurosporine, and qPCR were used to analyze levels of pri-miR-211-5p (top) and miR-211-5p (bottom) at 1, 3, and 6 h postexposure. (e) RCNs were cultured with RA, sevoflurane, etoposide, or staurosporine followed by 10 μg/mL α-Am; qPCR was then used to analyze levels of pri-miR-211-5p (top) and miR-211-5p (bottom) at 1, 3, and 6 h after α-Am treatment. (f, g) RCNs were transfected with miR-Ctrl or miR-211-5p mimics. (f) LDH release and (g) CC-3 activity were measured 24 h later. (h, i) RCNs were transfected with AntimiR-Ctrl or AntimiR-211-5p and then treated with RA, sevoflurane, etoposide, or staurosporine. (h) LDH release and (i) CC-3 activity were measured 24 h later. Data shown as means ± SDs. All in vitro experiments: 3 biological replicates × 3 technical replicates. *$p < .05$, **$p < .01$ (two-way ANOVA [condition × treatment] with Tukey post-hoc test).

Abbreviations: qPCR = quantitative polymerase chain reaction; RA = room air; RCNs = rat cortical neurons; α-Am = α-amanitin; LDH = lactate dehydrogenase; CC-3 = cleaved caspase-3; ANOVA = analysis of variance; AntimiR-211-5p = miR-211-5p hairpin inhibitor.
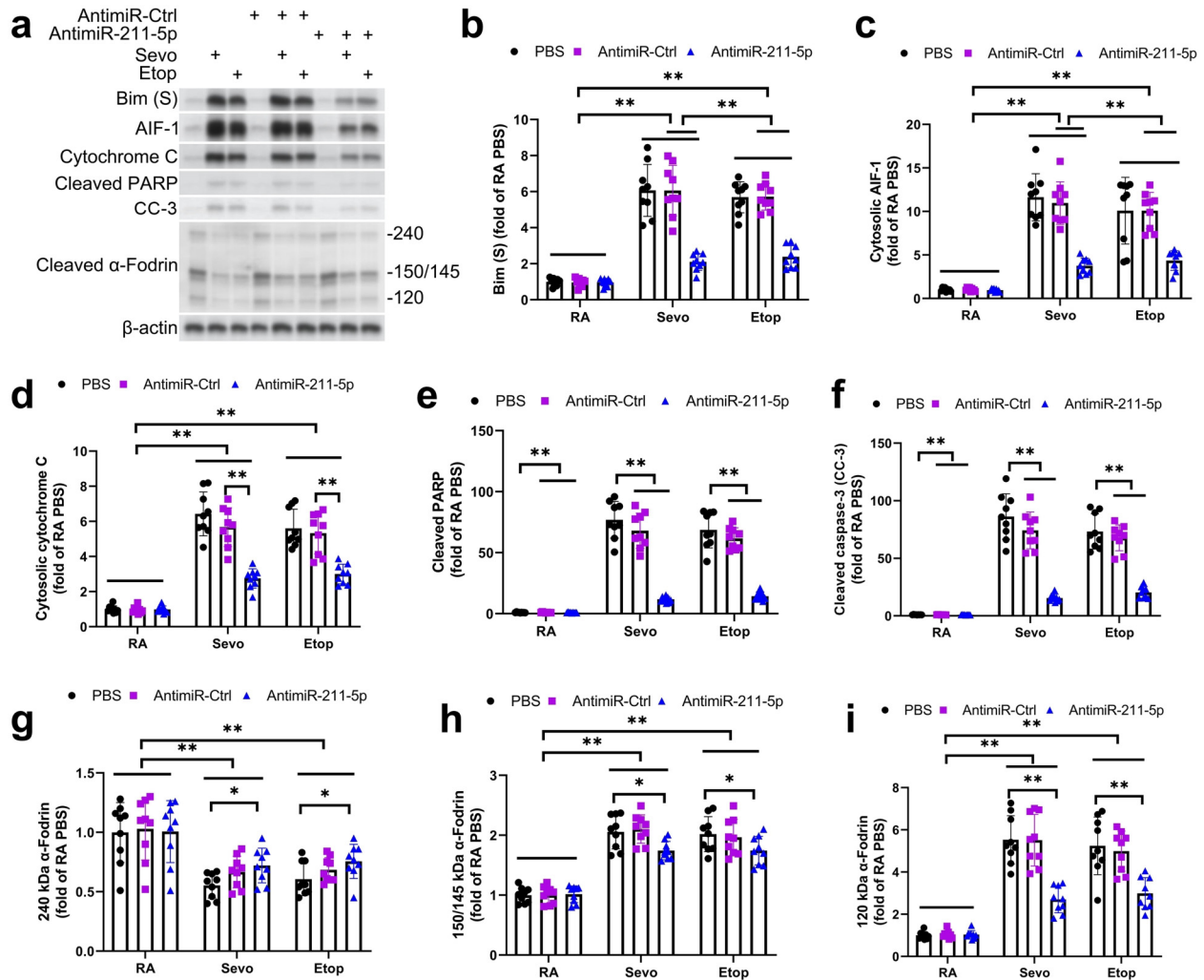
Figure 2. Sevoflurane-induced neuronal apoptosis rescued by AntimiR-211-5p. Primary RCNs were transfected with AntimiR-Ctrl or AntimiR-211-5p and then cultured with RA, sevoflurane, or etoposide. (a) Representative Western blot analysis of Bim, AIF-1, cytochrome C, cleaved PARP, CC-3, and α-fodrin (normalized to β-actin). (b–i) Quantification of whole cell lysate protein levels of (b) Bim, (c) AIF-1 (cytosolic fraction only), (d) cytochrome C (cytosolic fraction only), (e) cleaved PARP, (f) CC-3, (g) 240 kDa α-fodrin, (h) 150/145 kDa α-fodrin, and (i) 120 kDa α-fodrin. Data shown as means ± SDs. All in vitro experiments: 3 biological replicates × 3 technical replicates. *$p < .05$, **$p < .01$ (two-way ANOVA [condition × treatment] with Tukey post-hoc test).
Abbreviations: AntimiR-211-5p = miR-211-5p hairpin inhibitor; RA = room air; RCNs = rat cortical neurons; AIF-1 = allograft inflammatory factor 1; α-Am = α-amanitin; LDH = lactate dehydrogenase; CC-3 = cleaved caspase-3; ANOVA = analysis of variance; PARP = poly-(ADP-ribose) polymerase.

increased Bim protein expression and cytosolic release of cytochrome C and allograft inflammatory factor 1 (AIF-1), which were abrogated by AntimiR-211-5p (Figure 2b to d). Sevoflurane exposure also increased levels of cleaved poly-(ADP-ribose) polymerase (PARP) and CC-3, which were abrogated by AntimiR-211-5p (Figure 2e and f). Sevoflurane exposure increased levels of full-length α-fodrin (240 kDa) as well as the caspase-dependent cleaved α-fodrin fragment (150/120 kDa) and the calpain-dependent cleaved α-fodrin fragment (150/145 kDa) (Siman et al., 2004), which were abrogated by AntimiR-211-5p (Figure 2g to i). A similar pattern of findings were found in the positive control etoposide model (Figure 2a to i).

Sevoflurane-Induced Dysregulation of the miR-211-5p Target Efemp2 and Smad2/3 Signaling Rescued by AntimiR-211-5p In Vitro

Hippocampi from sevoflurane-exposed mice display Efemp2 downregulation (Hayase et al., 2016), and TargetScan analysis in mice, rats, and humans identified the 3′-UTR of Efemp2 mRNA as a putative, conserved target of miR-211-5p (Supplemental Figure S1). This evidence led us to hypothesize that Efemp2 may be a regulatory target of miR-211-5p in cortical neurons. Therefore, the murine Efemp2 3′-UTR sequence was inserted into a pmirGLO plasmid backbone (pmir-Efemp2) in order to investigate miR-211-5p's

regulation of Efemp2 mRNA expression. RCNs were co-transfected with pmir-Efemp2 or pmirGLO as well as miR-Ctrl or miR-211-5p mimics. miR-211-5p was shown to decrease luciferase activity in pmir-Efemp2-transfected cells 24 h after transfection; no changes were shown with the pmirGLO-transfected cells or miR-Ctrl-transfected cells (Figure 3a). These results show that the 3′-UTR of Efemp2 mRNA is directly targeted by miR-211-5p.

RNA-induced silencing complex (RISC) is formed by binding of Argonaute 2 (Ago2) proteins to one strand of mature miRNA, which is used as a template in order to recognize and subsequently cleave complementary mRNA (Becker et al., 2019). Therefore, miRNA:mRNA target pairs, such as the miR-211-5p:Efemp2 dyad, can be confirmed by Ago2-associated RNA immunoprecipitation (RIP). RCNs were harvested 6 h postsevoflurane treatment (the time point with the highest miR-211-5p expression) and underwent RIP with Ago2 antibodies. Significant enrichment of Efemp2 and miR-211-5p mRNA in the RISC complex were revealed with qPCR after sevoflurane exposure (Figure 3b). A similar pattern of findings were found in the positive control etoposide model (Figure 3b). These results show that sevoflurane enhances the RISC-based interaction of miR-211-5p and Efemp2 mRNA.

In vivo, qPCR revealed a decrease in cortical Efemp2 expression as early as 1 h postsevoflurane exposure; this decrease peaked at 24 h and was maintained at 72 h postsevoflurane exposure (Figure 3c). In vitro, qPCR analysis in RCNs showed a similar decrease in Efemp2 expression postsevoflurane exposure (Figure 3d). A similar pattern of findings were found in the positive control etoposide model (Figure 3d).

As Efemp2 encodes the ECM protein Fibulin-4, a negative regulator of Tgf-β/Smad signaling in murine neurons (Hanada et al., 2007; McLaughlin et al., 2006) and human fibroblasts (Renard et al., 2010; Urban & Davis, 2014), the role of miR-211-5p in the Efemp2/Tgf-β/Smad signaling pathway was assessed in RCNs postsevoflurane exposure. Expression of Efemp2 was decreased, while Smad2 and Smad3 phosphorylation were increased, after sevoflurane exposure (Figure 3e to h). These sevoflurane-induced changes were rescued by AntimiR-211-5p (Figure 3e to h). Expression of pro-apoptotic AIF-1 in nuclear fractions was enhanced after sevoflurane exposure, which was abrogated by AntimiR-211-5p (Figure 3i and j). A similar pattern of findings were found in the positive control etoposide model (Figure 3e to j).

The Neuroprotective Effects of AntimiR-211-5p are Mediated by Efemp2

Small-interfering RNA (siRNA)-based Efemp2 knockdown was used to investigate the role of Efemp2 in AntimiR-211-5p's neuroprotective effects. Three siRNAs against Efemp2 were tested, and the most potent siRNA

was selected for further experimentation (Supplemental Figure S2a). Sevoflurane induced LDH release from RCNs; this was not affected by the addition of Efemp2-specific small-interfering RNA (siEfemp2) (Supplemental Figure S2b). AntimiR-211-5p decreased sevoflurane-induced LDH release; notably, this effect was nullified by the addition of siEfemp2 (Supplemental Figure S2c). A similar pattern of findings were found in the positive control etoposide model (Supplemental Figure S2a to c).

The role of Efemp2 in AntimiR-211-5p's regulation of the Efemp2/Tgf-β/Smad signaling pathway was assessed in RCNs post-sevoflurane exposure. AntimiR-211-5p rescued sevoflurane-induced downregulation of Efemp2 and upregulation of Smad2 and Smad3 phosphorylation (Supplemental Figure S2d and e). These AntimiR-211-5p-induced changes were nullified by the addition of siEfemp2 (Supplemental Figure S2d and e). A similar pattern of findings were found in the positive control etoposide model (Supplemental Figure S2d and f).

AntimiR-211-5p Upregulates Efemp2 Expression, Downregulates Smad2/3 Signaling, and Reduces Apoptosis in Sevoflurane-Exposed Mouse Cortices

Vehicle (PBS), AntimiR-Ctrl, or AntimiR-211-5p was administered to room air-exposed or sevoflurane-exposed mice by i.c.v. injection 15 min postprocedure. Western blot analysis was then used to assess Efemp2 expression and Smad2/3 phosphorylation 24 h postroom air or sevoflurane exposure. Levels of Efemp2 were significantly decreased, and phosphorylated Smad2 and Smad3 were significantly increased, following sevoflurane exposure (Figure 4a and b). These results suggest that the regulation of Smad2/3 postsevoflurane exposure is via Tgf-β1-dependent phosphorylation rather than changes in the expression of Smad2/3. Treatment with AntimiR-211-5p rescued these changes in Efemp2 expression and Smad2/3 phosphorylation (Figure 4a and b).

We next investigated the effect of AntimiR-211-5p on apoptotic marker levels in the sevoflurane murine model. We revealed sevoflurane-induced upregulation of two Bim isoforms (small [S] and large [L]) but were not able to detect the presence of the Bim EL isoform. AntimiR-211-5p rescued sevoflurane-induced Bim (S) upregulation (Figure 4a and c). The expression of AIF-1 and cytochrome C were not altered by either sevoflurane or AntimiR-211-5p (Figure 4d to g), which reflects earlier work (Sabirzhanov et al., 2014). However, sevoflurane did induce nuclear AIF-1 translocation and mitochondrial release of cytochrome C, which were rescued by AntimiR-211-5p (Figure 4d to g). Moreover, AntimiR-211-5p rescued sevoflurane-induced cleavage of α-fodrin (150/145 kDa fragments) (Figure 4h and i). No discernible changes in the expression of 240 kDa α-fodrin or 120 kDa α-fodrin fragments were revealed in
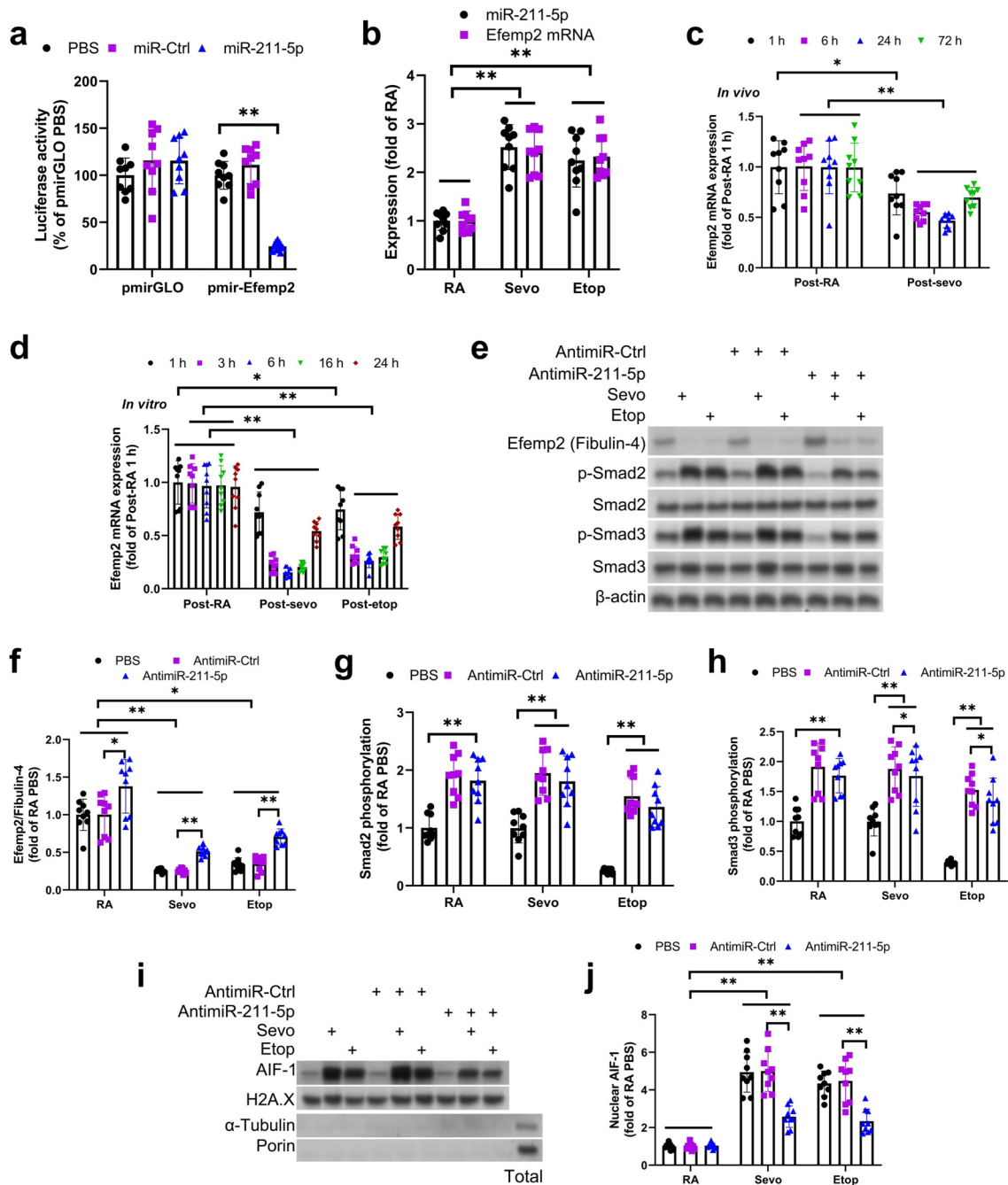
Figure 3. Sevoflurane-induced dysregulation of the miR-211-5p target Efemp2 and Smad2/3 signaling rescued by AntimiR-211-5p. (a) Primary RCNs were transfected with pmir-Efemp2 reporter or control reporter (pmirGLO) plasmid and co-transfected with miR-Ctrl or miR-211-5p mimic. Luciferase activity was assessed 24 h posttransfection. (b) Ago2-associated RIP qPCR analysis of Efemp2 and miR-211-5p levels in RCNs after treatment with RA, sevoflurane, or etoposide. (c) qPCR quantification of in vivo cortical Efemp2 mRNA levels 72 h following RA or sevoflurane exposure ($n = 9$ mice per cohort). (d) qPCR quantification of in vitro Efemp2 mRNA levels in primary RCNs after treatment with RA, sevoflurane, or etoposide. (e–j) RCNs were transfected with miR-Ctrl or miR-211-5p mimics and treated with RA, sevoflurane, or etoposide. After 24 h, Western blot analysis was carried out for (e) Efemp2, p-Smad2, Smad2, p-Smad3, and Smad3 in the cytosolic fractions (normalized to β-actin), and (i) AIF-1 (normalized to H2A.X) in the nuclear fractions showing negligible total expression of α-tubulin and porin from aggregated nuclear fractions. Quantification of (f) Efemp2 protein levels, (g, h) p-Smad2/Smad2 and p-Smad3/Smad3, and (i) nuclear AIF-1 protein levels. Data shown as means ± SDs. All in vitro experiments: 3 biological replicates × 3 technical replicates. *$p < .05$, **$p < .01$ (two-way ANOVA [condition × treatment] with Tukey post-hoc test).

Abbreviations: AntimiR-211-5p = miR-211-5p hairpin inhibitor; RA = room air; RCNs = rat cortical neurons; AIF-1 = allograft inflammatory factor 1; α-Am = α-amanitin; LDH = lactate dehydrogenase; Ago2 = Argonaute 2; CC-3 = cleaved caspase-3; ANOVA = analysis of variance; PARP = poly-(ADP-ribose) polymerase; qPCR = quantitative polymerase chain reaction; RIP = RNA immunoprecipitation .
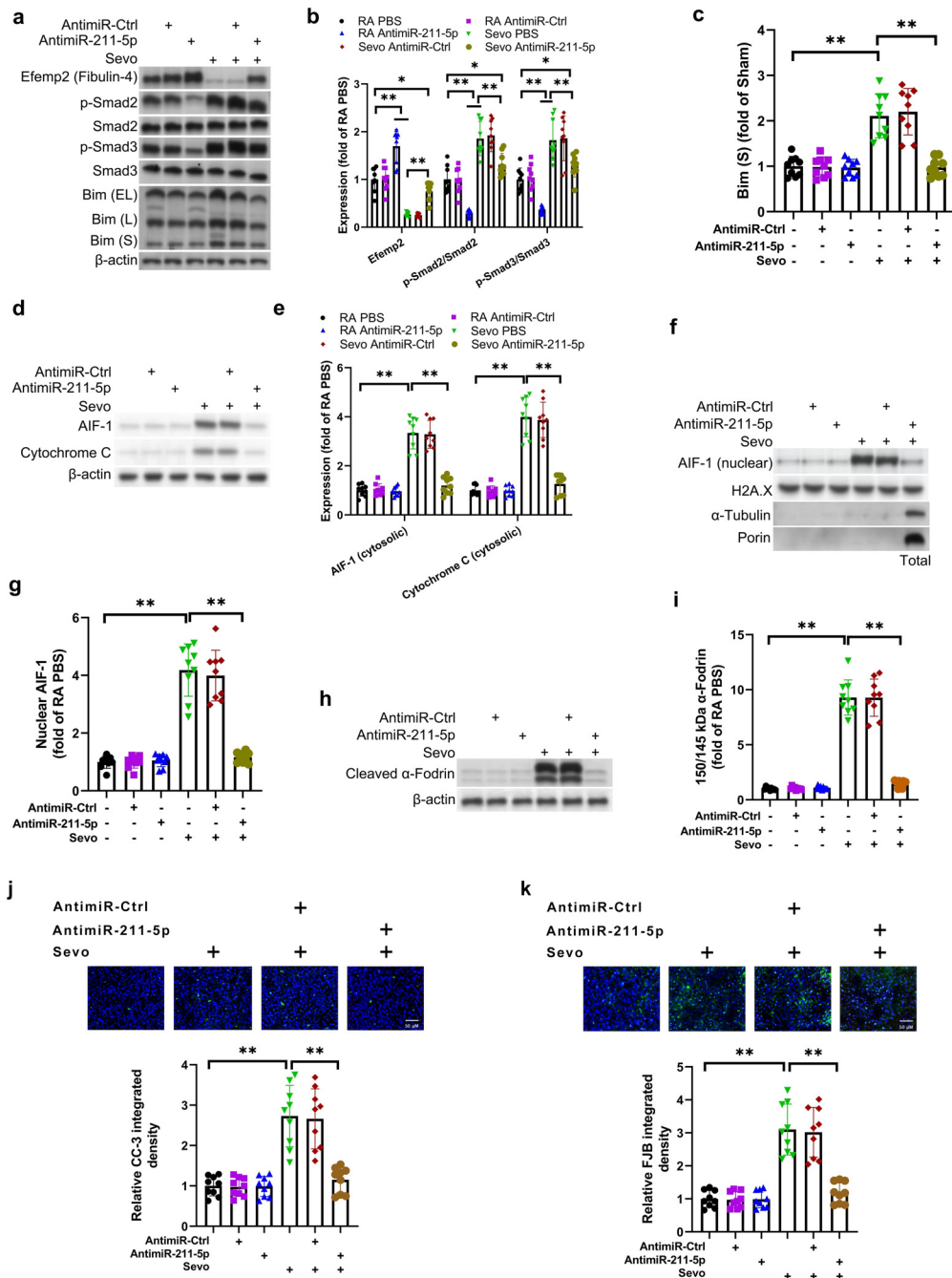
Figure 4. AntimiR-211-5p upregulates Efemp2 expression, downregulates Smad2/3 signaling, and reduces apoptotic marker expression in sevoflurane-exposed mouse cortices. (a–i) Western blot analysis of cortical whole tissue lysates from room air (RA)-exposed or sevoflurane-exposed mice treated with AntimiR-Ctrl or AntimiR-211-5p ($n = 9$ mice per cohort). Western blot analyses of (a) Efemp2, p-Smad2, Smad2, p-Smad3, Smad3, Bim (Bim small (S), 12 kDa, Bim large (L), 15 kDa, and Bim extra-large isoform (EL), 25 kDa) (normalized to β-actin). Quantification of (b) Efemp2 protein levels, p-Smad2/Smad2 and p-Smad3/Smad3, and (c) Bim S protein levels. Western blot analyses and quantification of (d, e) cytochrome C and AIF-1 protein expression (cytosolic fraction only) (normalized to β-actin), (f, g) AIF-1 expression (nuclear fraction only) (normalized to H2A.X) showing negligible total expression of α-tubulin and porin from aggregated nuclear fractions, and (h, i) 150/145 kDa α-fodrin expression (whole cell lysate) (normalized to β-actin). (j, k) Immunofluorescence analyses of (j) CC-3 staining and (k) FJB-positive cell counts in cortical tissue sections from RA-exposed or sevoflurane-exposed mice treated with AntimiR-Ctrl or AntimiR-211-5p ($n = 9$ mice per cohort). Data shown as means ± SDs. *$p < .05$, **$p < .01$ (two-way ANOVA [condition × treatment] with Tukey post-hoc test).

Abbreviations: AntimiR-211-5p = miR-211-5p hairpin inhibitor; RA = room air; RCNs = rat cortical neurons; AIF-1 = allograft inflammatory factor 1; α-Am = α-amanitin; LDH = lactate dehydrogenase; Ago2 = Argonaute 2; CC-3 = cleaved caspase-3; ANOVA = analysis of variance; PARP = poly-(ADP-ribose) polymerase; FJB = Fluoro-Jade B; qPCR = quantitative polymerase chain reaction.

this study, which could indicate a difference in activation of proteases in in vivo and in vitro models.

In order to validate our immunoblot findings, we conducted immunofluorescence analyses in cortical sections from the sevoflurane murine model. We discovered sevoflurane-induced upregulation of the apoptotic marker CC-3 (Ye et al., 2017), which was rescued by AntimiR-211-5p (Figure 4j). Furthermore, cortical neuronal death was assessed through Fluoro-Jade B (FJB) staining (Min et al., 2017). Sevoflurane significantly increased FJB + cell counts, indicating enhanced cortical neuronal cell death (Figure 4k). AntimiR-211-5p rescued sevoflurane-induced increases in FJB + cell counts. This evidence indicates that AntimiR-211-5p therapy reduces apoptosis in sevoflurane-exposed mouse cortices.

AntimiR-211-5p Rectifies Near-Term Motor Function and Cognitive Deficits Induced by Sevoflurane Exposure

Vehicle (PBS), AntimiR-Ctrl, or AntimiR-211-5p was administered to room air-exposed or sevoflurane-exposed mice by i.c.v. injection 15 min postprocedure. Then, several tests for motor and cognitive function were administered. The beam walk test was used immediately prior to sevoflurane exposure (day 0) and on days 1, 7, 14, 21, and 28 postexposure in order to investigate motor function. There were significant differences between the sevoflurane-exposed AntimiR-Ctrl and sham groups solely on days 1 and 7 postsevoflurane exposure (Figure 5a), indicating that sevoflurane adversely affects near-term motor function. Of note, AntimiR-211-5p therapy rescued this effect in sevoflurane-exposed mice.

In order to assess spatial working memory, the Y-maze spontaneous alternation test was used immediately prior to sevoflurane exposure (day 0) and on days 1, 7, 14, 21, and 28 postexposure. A functional working memory was found in the sham mouse group on day 1 postexposure ($81.4 \pm 3.3\%$ spontaneous alternation) (Figure 5b). However, spontaneous alternation was significantly decreased solely on day 1 postexposure in sevoflurane-exposed AntimiR-Ctrl mice ($64.9 \pm 2.0\%$). Of note, AntimiR-211-5p therapy rescued this effect in sevoflurane-exposed mice. In order to further assess spatial working memory, the Morris water maze (MWM) test was used immediately prior to sevoflurane exposure (day 0) and on days 1–5 (first trial) and days 10–14 (second trial) post-exposure. Over days 1–4 (first trial), there were significant increases in latency time required to find the hidden platform in sevoflurane-exposed AntimiR-Ctrl compared to sham mice, indicating that sevoflurane adversely affects spatial memory (Figure 5c). Notably, sevoflurane-exposed mice treated with AntimiR-211-5p partially rescued this increase in latency time. Similarly, during the first trial's probe test on day 5, we observed significantly higher latency times (Figure 5d), significantly lower number of crossings (Figure 5e), and

significantly lower times in the target quadrant (Figure 5f) in sevoflurane-exposed AntimiR-Ctrl compared to sham mice, effects partially rescued by AntimiR-211-5p (Figure 5d to f). However, these changes in sevoflurane-exposed mice were not observed during the second trial's probe test on day 14 (Figure 5d to f), suggesting that sevoflurane's observable effects are near-term.

The NOR test was then used to assess retention memory on days 2–3 postsevoflurane exposure (Figure 5g and h). An intact memory was revealed in sham mice, who spent 15 s with the novel object during the choice phase on day 3 post-sevoflurane exposure (Figure 5h). Sevoflurane-exposed mice treated with AntimiR-Ctrl or AntimiR-211-5p spent a similar time with the novel object compared to the sham group (Figure 5h), suggesting that sevoflurane has no observable effects on retention memory.

Discussion

As miRNAs are able to target a number of mRNAs, they are able to exert a large degree of control over gene expression within the brain (Henshall, 2014; Ponomarev et al., 2013). This study aimed to investigate whether postsevoflurane neuronal apoptosis and cognitive deficits could be better controlled via modification of miR-211-5p expression. We found that both in vitro sevoflurane exposure resulted in a rapid increase in miR-211-5p expression, while AntimiR-211-5p reduced sevoflurane-induced neuronal apoptosis. AntimiR-211-5p also promoted a reduction in markers of caspase-independent apoptosis (AIF-1 nuclear translocation) (Susin et al., 1999) and -dependent apoptosis (PARP, CC-3, and α-fodrin cleavage) (Siman et al., 2004), mitochondrial permeabilization, and expression of Bim. In fact, treatment of neuronal cells with miR-211-5p mimics alone induces apoptosis, indicating that miR-211-5p can independently drive the neuronal cell death pathway. These in vitro findings were validated by two in vitro neuronal apoptosis models: the protein kinase inhibitor staurosporine and DNA-damaging agent etoposide, which respectively promote mitochondrial release of cytochrome C and AIF-1 via caspase-independent and -dependent mechanisms (Yakovlev et al., 2004).

miR-211-5p has been previously shown to impair murine neuronal viability as well as neurite growth and branching by directly downregulating the pro-neurogenic Nua kinase Nuak1, thereby accelerating neuronal loss and cognitive dysfunction (Fan et al., 2016). However, pro-neurogenic Nuak1 expression is paradoxically upregulated in the murine hippocampus following sevoflurane exposure (Hayase et al., 2016), suggesting that miR-211-5p's negative regulation of Nuak1 does not play a significant role in sevoflurane-induced neuronal loss and cognitive dysfunction. On the other hand, Efemp2 (encoding the ECM protein Fibulin-4) has previously been identified as a target of miR-211-5p in chondrocytes (Liu & Luo, 2019). Although Efemp2 is overexpressed in glioma
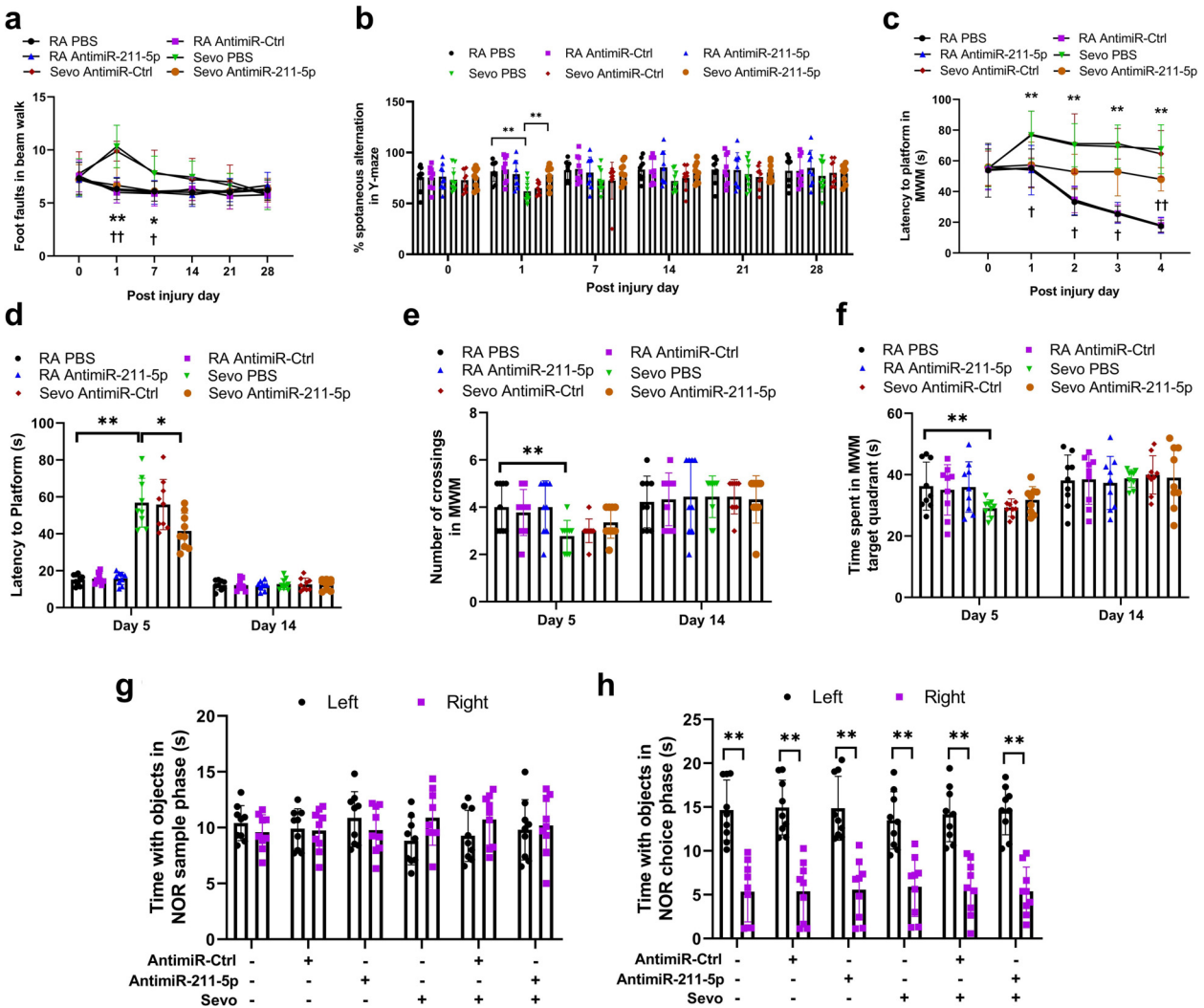
Figure 5. AntimiR-211-5p rectifies near-term motor function and cognitive deficits induced by sevoflurane exposure. (a) Beam walk analysis for fine motor coordination and balance and (b) Y-maze spontaneous alternation analysis for spatial working memory function on days 0 (pre-exposure), 1, 7, 14, 21, and 28 in RA-exposed or sevoflurane-exposed mice treated with AntimiR-Ctrl or AntimiR-211-5p ($n = 9$ mice per cohort). All mice had ≤10-foot faults prior to RA or sevoflurane exposure. (c–f) MWM analysis for spatial memory function ($n = 9$ mice per cohort). Quantification of (c) escapes latency during the first four days after sevoflurane exposure as well as (d) escape latency, (e) number of crossings, and (f) time spent in the target quadrant during probe test on the fifth day (first test) and fourteenth day (second test) post-RA or sevoflurane exposure. (g, h) NOR, (g) sample phase, and (h) choice phase assessments for memory retention on days 2–3 post-RA or sevoflurane exposure ($n = 9$ mice per cohort). Data shown as means ± SDs. *$p < .05$, **$p < .01$ (two-way ANOVA [condition × treatment] with Tukey post-hoc test).

Abbreviations: AntimiR-211-5p = miR-211-5p hairpin inhibitor; RA = room air; MWM = Morris water maze; NOR = novel object recognition; ANOVA = analysis of variance.

tumor cells and plays an anti-apoptotic role in glioma cells (Wang et al., 2015), Efemp2's regulatory role in injury-induced neuronal apoptosis has not been investigated. Here, we found a rapid reduction in Efemp2 expression following sevoflurane exposure, which was validated in our etoposide model. We also found that Efemp2 downregulation is associated with increased Smad2/3 phosphorylation, Bim upregulation, and nuclear translocation of AIF-1, leading to neuronal apoptosis (Cregan et al., 2004). Our findings are

consistent with previous studies showing that Efemp2 knockdown promotes Smad2/3 phosphorylation (Hanada et al., 2007; McLaughlin et al., 2006) and that enhanced Smad2/3 phosphorylation promotes pro-apoptotic Bim expression (Ramesh et al., 2008; Thi et al., 2013).

Of note, significantly enriched levels of Efemp2 and miR-211-5p were revealed within the RISC complex, suggesting that posttranscriptional Efemp2 mRNA processing is miR-dependent. Efemp2 downregulation coupled with

nuclear translocation of AIF-1 by AntimiR-211-5p indicates a key role for the miR-211-5p/Efemp2 axis in neuronal cell death. Furthermore, Efemp2 silencing was able to reverse AntimiR-211-5p-dependent neuroprotection. Mature miRNA catabolism is relatively variable with a quick turnover rate compared to its processing, which is constant (Krol et al., 2010). The rate of miR-211-5p catabolism in RCNs was shown to be fast, and the rate of decay was not affected by cellular injury. Exposure to sevoflurane (or etoposide) resulted in increased levels of α-Am-inhibitable pri-miR-211 and miR-211-5p expression, which suggests that a higher rate of pri-miR-211 transcription is the cause of sevoflurane-induced miR-211-5p upregulation. Further investigation is needed into the mechanism involved in the upregulated transcription of miR-211-5p, and possibly its host gene transient receptor potential cation channel subfamily M member 1 (Levy et al., 2010), following sevoflurane exposure.

We also found that in vivo sevoflurane exposure resulted in a rapid increase in miR-211-5p expression. The role of miR-211-5p in the promotion of in vivo sevoflurane-induced neuronal apoptosis was indicated by the neuroprotective effects exerted with AntimiR-211-5p. This treatment resulted in a reduction in sevoflurane-dependent activation of Bim and other downstream targets in the injured murine cortex. This was associated with a decrease in sevoflurane-induced α-fodrin cleavage, mitochondrial release of cytochrome C and AIF-1, CC-3 expression, and cortical neuronal death. Furthermore, we revealed an amelioration of near-term motor and cognitive functional deficits with AntimiR-211-5p therapy. Significant improvements in motor and cognitive parameters after treatment with the AntimiR-211-5p were found on days 1–7 postsevoflurane exposure.

There have been limited reports on the impact of sevoflurane anesthesia on levels of Efemp2 expression. Profound downregulation of Efemp2 has been reported by one murine study (Hayase et al., 2016), whereas one rat study reported no significant changes in Efemp2 expression (Pan et al., 2011). However, these previous studies performed no further experiments on Efemp2's role in sevoflurane exposure. This study is the first to reveal that sevoflurane exposure results in the reduction of Efemp2 mRNA and protein expression in the injured murine cortex and that neuronal Efemp2 may provide neuroprotection from sevoflurane exposure.

In conclusion, this study revealed the significance of sevoflurane-induced increases in miR-211-5p on the promotion of neuronal apoptosis via inhibition of Efemp2 and its downstream targets.

Author's Contributions

Conceived and designed the study: M.Z., Y.S., T.Z., X.L.; Performed the literature search and data extraction: Y.S., Y.L., X.L., W.Z.; Analyzed the data: Y.S., D.Z.; Drafted the manuscript: Y.S., Y.L.

References

Backeljauw, B., Holland, S. K., Altaye, M., & Loepke, A. W. (2015). Cognition and brain structure following early childhood surgery with anesthesia. *Pediatrics*, *136*(1), e1–e12. https://doi.org/10.1542/peds.2014-3526

Becker, W. R., Ober-Reynolds, B., Jouravleva, K., Jolly, S. M., Zamore, P. D., & Greenleaf, W. J. (2019). High-throughput analysis reveals rules for target RNA binding and cleavage by AGO2. *Molecular Cell*, *75*(4), 741–755. e11. https://doi.org/10.1016/j.molcel.2019.06.012

Brioni, J. D., Varughese, S., Ahmed, R., & Bein, B. (2017). A clinical review of inhalation anesthesia with sevoflurane: From early research to emerging topics. *Journal of Anesthesia*, *31*(5), 764–778. https://doi.org/10.1007/s00540-017-2375-6

Chen, G., Gong, M., Yan, M., & Zhang, X. (2013). Sevoflurane induces endoplasmic reticulum stress mediated apoptosis in hippocampal neurons of aging rats. *PLoS One*, *8*(2), e57870. https://doi.org/10.1371/journal.pone.0057870

Cregan, S. P., Dawson, V. L., & Slack, R. S. (2004). Role of AIF in caspase-dependent and caspase-independent cell death. *Oncogene*, *23*(16), 2785. https://doi.org/10.1038/sj.onc.1207517

Cunha-Oliveira, T., Rego, A. C., Cardoso, S. M., Borges, F., Swerdlow, R. H., & Macedo, T. (2006). Mitochondrial dysfunction and caspase activation in rat cortical neurons treated with cocaine or amphetamine. *Brain Research*, *1089*(1), 44–54. https://doi.org/10.1016/j.brainres.2006.03.061

Fan, C., Wu, Q., Ye, X., Luo, H., Yan, D., & Xiong, Y. (2016). Role of miR-211 in neuronal differentiation and viability: Implications to pathogenesis of Alzheimer's disease. *Frontiers in Aging Neuroscience*, *8*, 166.

Fujimoto, S., Ishikawa, M., Nagano, M., & Sakamoto, A. (2015). Influence of neonatal sevoflurane exposure on nerve development-related microRNAs and behavior of rats. *Biomedical Research*, *36*(6), 347–355. https://doi.org/10.2220/biomedres.36.347

Hanada, K., Vermeij, M., Garinis, G. A., De Waard, M. C., Kunen, M. G., & Myers, L. (2007). Perturbations of vascular homeostasis and aortic valve abnormalities in fibulin-4 deficient mice. *Circulation Research*, *100*(5), 738–746. https://doi.org/10.1161/01.RES.0000260181.19449.95

Hayase, T., Tachibana, S., & Yamakage, M. (2016). Effect of sevoflurane anesthesia on the comprehensive mRNA expression profile of the mouse hippocampus. *Medical Gas Research*, *6*(2), 70. https://doi.org/10.4103/2045-9912.184715

Henshall, D. C. (2014). MicroRNA and epilepsy: Profiling, functions and potential clinical applications. *Current Opinion in Neurology*, *27*(2), 199. https://doi.org/10.1097/WCO.0000000000000079

Jiang, J., Lv, X., Wu, X., Yang, Y., & Jiang, H. (2017). Downregulation of circulating insulin-like growth factor 1 contributes to memory impairment in aged mice after sevoflurane anesthesia. *Behavioural Pharmacology*, *28*(2), 238–243. https://doi.org/10.1097/FBP.0000000000000293

Jimenez-Mateos, E., & Henshall, D. (2013). Epilepsy and microRNA. *Neuroscience*, *238*, 218–229. https://doi.org/10.1016/j.neuroscience.2013.02.027

Krol, J., Busskamp, V., Markiewicz, I., Stadler, M. B., Ribi, S., & Richter, J. (2010). Characterizing light-regulated retinal microRNAs reveals rapid turnover as a common property of neuronal microRNAs. *Cell*, *141*(4), 618–631. https://doi.org/10.1016/j.cell.2010.03.039

Levy, C., Khaled, M., Iliopoulos, D., Janas, M. M., Schubert, S., & Pinner, S. (2010). Intronic miR-211 assumes the tumor suppressive function of its host gene in melanoma. *Molecular Cell*, *40*(5), 841–849. https://doi.org/10.1016/j.molcel.2010.11.020

Liu, H., & Luo, J. (2019). miR-211-5p contributes to chondrocyte differentiation by suppressing fibulin-4 expression to play a role in osteoarthritis. *The Journal of Biochemistry*, *166*(6), 495–502. https://doi.org/10.1093/jb/mvz065

Liu, Y., Pan, N., Ma, Y., Zhang, S., Guo, W., & Li, H. 2013a). Inhaled sevoflurane may promote progression of amnestic mild cognitive impairment: A prospective, randomized parallel-group study. *The American Journal of the Medical Sciences*, *345*(5), 355–360. https://doi.org/10.1097/MAJ.0b013e31825a674d

Liu, S., Paule, M. G., Zhang, X., Newport, G. D., Apana, S. M., & Berridge, M. S. 2013b). The evaluation of sevoflurane-induced apoptotic neurodegeneration with microPET using [18F]-DFNSH in the developing rat brain. *Journal of Drug and Alcohol Research*, *2*(7).

Liu, D.-Z., Tian, Y., Ander, B. P., Xu, H., Stamova, B. S., & Zhan, X. (2010). Brain and blood microRNA expression profiling of ischemic stroke, intracerebral hemorrhage, and kainate seizures. *Journal of Cerebral Blood Flow & Metabolism*, *30*(1), 92–101. https://doi.org/10.1038/jcbfm.2009.186

McLaughlin, P. J., Chen, Q., Horiguchi, M., Starcher, B. C., Stanton, J. B., & Broekelmann, T. J. (2006). Targeted disruption of fibulin-4 abolishes elastogenesis and causes perinatal lethality in mice. *Molecular and Cellular Biology*, *26*(5), 1700–1709. https://doi.org/10.1128/MCB.26.5.1700-1709.2006

Min, S.-J., Hyun, H.-W., & Kang, T.-C. (2017). Leptomycin B attenuates neuronal death via PKA- and PP2B-mediated ERK1/2 activation in the rat hippocampus following status epilepticus. *Brain Research*, *1670*, 14–23. https://doi.org/10.1016/j.brainres.2017.06.002

Nassogne, M. C., Evrard, P., & Courtoy, P. J. (1998). Selective direct toxicity of cocaine on fetal mouse neurons: Teratogenic implications of neurite and apoptotic neuronal loss. *Annals of the New York Academy of Sciences*, *846*(1), 51–68. https://doi.org/10.1111/j.1749-6632.1998.tb09726.x

Pan, Z., Lu, X.-F., Shao, C., Zhang, C., Yang, J., & Ma, T. (2011). The effects of sevoflurane anesthesia on rat hippocampus: A genomic expression analysis. *Brain Research*, *1381*, 124–133. https://doi.org/10.1016/j.brainres.2011.01.020

Ponomarev, E. D., Veremeyko, T., & Weiner, H. L. (2013). MicroRNAs are universal regulators of differentiation, activation, and polarization of microglia and macrophages in normal and diseased CNS. *Glia*, *61*(1), 91–103. https://doi.org/10.1002/glia.22363

Qiao, Y., Feng, H., Zhao, T., Yan, H., Zhang, H., & Zhao, X. (2015). Postoperative cognitive dysfunction after inhalational anesthesia in elderly patients undergoing major surgery: The influence of anesthetic technique, cerebral injury and systemic inflammation. *BMC Anesthesiology*, *15*(1), 154. https://doi.org/10.1186/s12871-015-0130-9

Qiu, J., Shi, P., Mao, W., Zhao, Y., Liu, W., & Wang, Y. (2015). Effect of apoptosis in neural stem cells treated with sevoflurane. *BMC Anesthesiology*, *15*(1), 25. https://doi.org/10.1186/s12871-015-0018-8

Ramesh, S., Qi, X. J., Wildey, G. M., Robinson, J., Molkentin, J., & Letterio, J. (2008). TGFβ-mediated BIM expression and apoptosis are regulated through SMAD3-dependent expression of the MAPK phosphatase MKP2. *EMBO Reports*, *9*(10), 990–997. https://doi.org/10.1038/embor.2008.158

Redell, J. B., Liu, Y., & Dash, P. K. (2009). Traumatic brain injury alters expression of hippocampal microRNAs: Potential regulators of multiple pathophysiological processes. *Journal of Neuroscience Research*, *87*(6), 1435–1448. https://doi.org/10.1002/jnr.21945

Renard, M., Holm, T., Veith, R., Callewaert, B. L., Adès, L. C., & Baspinar, O. (2010). Altered TGFβ signaling and cardiovascular manifestations in patients with autosomal recessive cutis laxa type I caused by fibulin-4 deficiency. *European Journal of Human Genetics*, *18*(8), 895. https://doi.org/10.1038/ejhg.2010.45

Sabirzhanov, B., Stoica, B. A., Hanscom, M., Piao, C. S., & Faden, A. I. (2012). Over-expression of HSP70 attenuates caspase-dependent and caspase-independent pathways and inhibits neuronal apoptosis. *Journal of Neurochemistry*, *123*(4), 542–554. https://doi.org/10.1111/j.1471-4159.2012.07927.x

Sabirzhanov, B., Zhao, Z., Stoica, B. A., Loane, D. J., Wu, J., & Borroto, C. (2014). Downregulation of miR-23a and miR-27a following experimental traumatic brain injury induces neuronal cell death through activation of proapoptotic Bcl-2 proteins. *Journal of Neuroscience*, *34*(30), 10055–10071. https://doi.org/10.1523/JNEUROSCI.1260-14.2014

Satomoto, M., Satoh, Y., Terui, K., Miyao, H., Takishima, K., & Ito, M. (2009). Neonatal exposure to sevoflurane induces abnormal social behaviors and deficits in fear conditioning in mice. *Anesthesiology: The Journal of the American Society of Anesthesiologists*, *110*(3), 628–637.

Siman, R., McIntosh, T. K., Soltesz, K. M., Chen, Z., Neumar, R. W., & Roberts, V. L. (2004). Proteins released from degenerating neurons are surrogate markers for acute brain damage. *Neurobiology of Disease*, *16*(2), 311–320. https://doi.org/10.1016/j.nbd.2004.03.016

Sun, L. (2010). Early childhood general anaesthesia exposure and neurocognitive development. *British Journal of Anaesthesia*, *105*(suppl_1), i61–ii8. https://doi.org/10.1093/bja/aeq302

Susin, S. A., Lorenzo, H. K., Zamzami, N., Marzo, I., Snow, B. E., & Brothers, G. M. (1999). Molecular characterization of mitochondrial apoptosis-inducing factor. *Nature*, *397*(6718), 441. https://doi.org/10.1038/17135

Takaenoki, Y., Satoh, Y., Araki, Y., Kodama, M., Yonamine, R., & Yufune, S. (2014). Neonatal exposure to sevoflurane in mice causes deficits in maternal behavior later in adulthood. *Anesthesiology: The Journal of the American Society of Anesthesiologists*, *120*(2), 403–415.

Tao, G., Zhang, J., Zhang, L., Dong, Y., Yu, B., & Crosby, G. (2014). Sevoflurane induces tau phosphorylation and glycogen synthase kinase 3β activation in young mice. *Anesthesiology: The Journal of the American Society of Anesthesiologists*, *121*(3), 510–527.

Thi, H. T. H., Lim, H.-S., Kim, J., Kim, Y.-M., Kim, H.-Y., & Hong, S. (2013). Transcriptional and post-translational regulation of Bim is essential for TGF-β and TNF-α-induced apoptosis of gastric cancer cell. *Biochimica et Biophysica Acta (BBA)-General Subjects*, *1830*(6), 3584–3592. https://doi.org/10.1016/j.bbagen.2013.03.006

Urban, Z., & Davis, E. C. (2014). Cutis laxa: Intersection of elastic fiber biogenesis, TGFβ signaling, the secretory pathway and metabolism. *Matrix Biology*, *33*, 16–22. https://doi.org/10.1016/j.matbio.2013.07.006

Vutskits, L., & Xie, Z. (2016). Lasting impact of general anaesthesia on the brain: Mechanisms and relevance. *Nature Reviews Neuroscience*, *17*(11), 705. https://doi.org/10.1038/nrn.2016.128

Wang, L., Chen, Q., Chen, Z., Tian, D., Xu, H., & Cai, Q. (2015). EFEMP2 is upregulated in gliomas and promotes glioma cell proliferation and invasion. *International Journal of Clinical and Experimental Pathology*, *8*(9), 10385.

Yakovlev, A. G., Di Giovanni, S., Wang, G., Liu, W., Stoica, B., & Faden, A. I. (2004). BOK and NOXA are essential mediators of p53-dependent apoptosis. *Journal of Biological Chemistry*, *279*(27), 28367–28374. https://doi.org/10.1074/jbc.M313526200

Yang, Q., Yang, Z.-F., Liu, S.-B., Zhang, X.-N., Hou, Y., & Li, X.-Q. (2010). Neuroprotective effects of hydroxysafflor yellow A against excitotoxic neuronal death partially through down-regulation of NR2B-containing NMDA receptors. *Neurochemical Research*, *35*(9), 1353–1360. https://doi.org/10.1007/s11064-010-0191-6

Ye, X., Shen, T., Hu, J., Zhang, L., Zhang, Y., & Bao, L. (2017). Purinergic 2X7 receptor/NLRP3 pathway triggers neuronal apoptosis after ischemic stroke in the mouse. *Experimental Neurology*, *292*, 46–55. https://doi.org/10.1016/j.expneurol.2017.03.002

Ye, J., Zhang, Z., Wang, Y., Chen, C., Xu, X., & Yu, H. (2016). Altered hippocampal microRNA expression profiles in neonatal rats caused by sevoflurane anesthesia: MicroRNA profiling and bioinformatics target analysis. *Experimental and Therapeutic Medicine*, *12*(3), 1299–1310. https://doi.org/10.3892/etm.2016.3452

Yu, S., Yeh, C.-H., Strasser, U., Tian, M., & Choi, D. (1999). NMDA receptor-mediated K + efflux and neuronal apoptosis. *Science (New York, NY)*, *284*(5412), 336–339. https://doi.org/10.1126/science.284.5412.336

Yu, Y., Zhang, P., Yan, J., Sun, Y., Wu, X., & Xi, S. (2016). Sevoflurane induces cognitive impairments via the MiR-27b/LIMK1-signaling pathway in developing rats. *Inhalation Toxicology*, *28*(14), 731–738. https://doi.org/10.1080/08958378.2016.1266532

Zheng, S., An, L., Cheng, X., & Wang, Y. (2013). Sevoflurane causes neuronal apoptosis and adaptability changes of neonatal rats. *Acta Anaesthesiologica Scandinavica*, *57*(9), 1167–1174. https://doi.org/10.1111/aas.12163

Ziu, M., Fletcher, L., Rana, S., Jimenez, D. F., & Digicaylioglu, M. (2011). Temporal differences in microRNA expression patterns in astrocytes and neurons after ischemic injury. *PloS One*, *6*(2), e14724. https://doi.org/10.1371/journal.pone.0014724